

# Comparison of interfacial and electrical characteristics of HfO<sub>2</sub> and HfAlO high-*k* dielectrics on compressively strained Si<sub>1-x</sub>Ge<sub>x</sub>

K. K. S. Curreem, P. F. Lee, K. S. Wong, and J. Y. Dai<sup>a)</sup>

*Department of Applied Physics, The Hong Kong Polytechnic University, Hung Hom, Kowloon, Hong Kong, People's Republic of China*

M. J. Zhou, J. Wang, and Quan Li

*Department of Physics, The Chinese University of Hong Kong, Shatin, New Territory, Hong Kong, People's Republic of China*

(Received 17 January 2006; accepted 19 March 2006; published online 4 May 2006)

Interfacial reactions and electrical properties of HfO<sub>2</sub> and HfAlO high-*k* gate dielectric films on strained Si<sub>1-x</sub>Ge<sub>x</sub> (*x*=17%) fabricated by pulsed-laser deposition were investigated. The dielectric films were characterized by x-ray photoelectron spectroscopy, transmission electron microscopy, and electrical measurements. We found that alloying of HfO<sub>2</sub> with alumina can reduce the GeO<sub>x</sub> formation at the interfacial layer and thus reduce the Ge diffusion during the film post-thermal annealing process. Such suppression effect significantly improved the electrical properties of the dielectric films. © 2006 American Institute of Physics. [DOI: 10.1063/1.2201887]

In the semiconductor industry, there is an urgent demand for suitable high-*k* dielectric materials to replace SiO<sub>2</sub> as the gate dielectric in the future advanced complementary metal-oxide-semiconductor (CMOS) technology.<sup>1,2</sup> Recent literatures as well as our preliminary results have shown that HfO<sub>2</sub> is one promising high-*k* gate dielectric substitute for SiO<sub>2</sub> due to its thermodynamic stability and low leakage current.<sup>1-8</sup> However, the carrier mobility degradation due to the high-*k* gate dielectric induced phonon and Coulomb scattering effect limits the application of high-*k* gate dielectrics.<sup>2</sup> It has been noticed recently that the use of a compressively strained Si<sub>1-x</sub>Ge<sub>x</sub> surface channel may serve as a solution to the carrier mobility degradation problem.<sup>2,5,9-11</sup>

The main issue in the HfO<sub>2</sub>-Si<sub>1-x</sub>Ge<sub>x</sub> system is the interfacial reaction, in particular, the GeO<sub>x</sub> formation and Ge diffusion that result in large amounts of interfacial traps and charge traps in the dielectric.<sup>2,12-14</sup> In addition, the relatively low crystallization temperature (about 500 °C) and high oxygen diffusivity of HfO<sub>2</sub> result in a rough interfacial structure and a large leakage current. A good interface which is thermodynamically stable and has low density of states is therefore essential in reducing the scattering effect on the charge carriers in the channel.<sup>9,15,16</sup> It has been illustrated that adding alumina into HfO<sub>2</sub> on Si (forming HfAlO) increases its crystallization temperature and reduces the oxygen diffusivity.<sup>17</sup> However, to the best of our knowledge, there has not been any report demonstrating that HfAlO can also improve the interfacial reaction and electrical property when applied on the Si<sub>1-x</sub>Ge<sub>x</sub> surface channel MOS field effect transistor. In this letter, we report on synthesis and characterizations of HfAlO thin films, in comparison with HfO<sub>2</sub>, on compressively strained Si<sub>1-x</sub>Ge<sub>x</sub>. The reactions at the film-Si<sub>1-x</sub>Ge<sub>x</sub> interface and the corresponding electrical properties of the MOS capacitors are investigated.

Si substrates with a layer of 15 nm compressively strained *p*-type Si<sub>1-x</sub>Ge<sub>x</sub> (*x*=17%) on top were first cleaned with dilute hydrofluoric acid solution to remove the native

oxide from the surface. The dielectric films were then grown by pulsed-laser deposition (PLD) on the strained Si<sub>1-x</sub>Ge<sub>x</sub> layer with a base pressure of  $\sim 2 \times 10^{-4}$  Pa and an oxygen partial pressure of 2 Pa at 550 °C using HfO<sub>2</sub> and Al<sub>2</sub>O<sub>3</sub> composite target (Hf:Al=1:1). The postannealing was carried out in a N<sub>2</sub> ambient at 600 °C for 45 min. In order to investigate the interfacial chemical structure, another set of samples with very thin (about 1.5 nm) HfO<sub>2</sub> and HfAlO films were deposited on the same substrate for the x-ray photoelectron spectroscopy (XPS) analysis. Such thickness allows an XPS investigation of the film and the interface simultaneously, and thus information on interfacial reactions can be obtained. The interfacial microstructure was observed by transmission electron microscopy (TEM) using a JEOL 2010 electron microscope. For an electrical property characterization, thicker films with thicknesses of about 5 nm were deposited. The MOS capacitor structures on strained Si<sub>1-x</sub>Ge<sub>x</sub> were fabricated by depositing Pt dot electrodes for both as-grown and annealed samples. Both high-frequency (1 MHz) capacitance-voltage (*C-V*) measurement using an HP4194A impedance analyzer and current-voltage (*J-V*) measurement were carried out.

Figure 1(a) shows XPS spectra of the Hf 4*f* binding energies for the HfO<sub>2</sub> and HfAlO thin films before and after thermal annealing. The peak positions were calibrated using C 1*s* lines as the reference. For the as-grown samples, the two distinct peaks corresponding to the Hf 4*f*<sub>7/2</sub> and 4*f*<sub>5/2</sub> of the Hf-O bond are identical, while they become broaden and difficult to resolve for the annealed samples, especially the HfO<sub>2</sub> film. This peak broadening is due to the formation of Hf silicate or germanate at the interface during the thermal annealing.<sup>9</sup> The convolution of Hf silicate and/or germanate peaks with Hf 4*f* peaks results in the broadening of the Hf-O peaks. In addition, very clear differences in the Hf 4*f* peaks can be observed for the annealed HfO<sub>2</sub> and HfAlO films. We believe that the relatively less broadening effect for the annealed HfAlO film compared to that for the annealed HfO<sub>2</sub> film can be attributed to the fact that the presence of Al in the film reduces oxygen diffusion in the film and thus reduces the formation of Hf silicate and germanate at the interface.

<sup>a)</sup> Author to whom correspondence should be addressed; electronic mail: apdaijy@inet.polyu.edu.hk

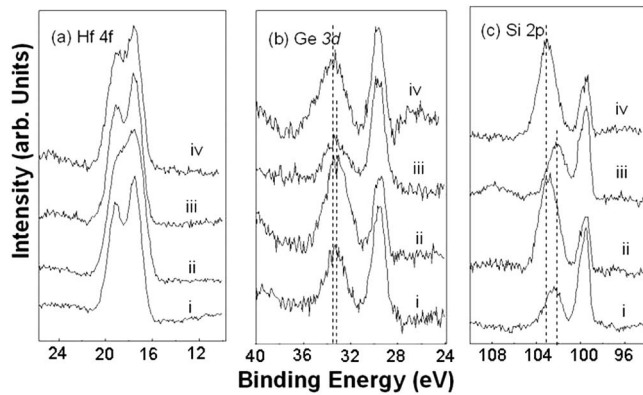


FIG. 1. XPS spectra of Hf 4f (a), Ge 3d (b), and Si 2p (c) binding energies for the films of HfO<sub>2</sub> as-grown (i), HfO<sub>2</sub> after annealed (ii), HfAlO as-grown (iii), and HfAlO after annealed (iv).

Figure 1(b) shows the XPS spectra of Ge 3d binding energies for the HfO<sub>2</sub> and HfAlO thin films before and after thermal annealing. Curve fittings of the Ge 3d core level spectra reveal two peaks corresponding to chemical bindings of Ge in elemental Ge and GeO<sub>x</sub>, respectively. The main peak at the binding energy of  $\sim 29.3$  eV originates from the elemental form of Ge in the Si<sub>1-x</sub>Ge<sub>x</sub> substrate, and the peak at the higher binding energy indicates the presence of GeO<sub>x</sub> resulting from the Ge oxidation at the interfacial region. By comparing the peak intensities between the as-grown and annealed HfO<sub>2</sub> samples, one can find the significant increment of the GeO<sub>x</sub> peak intensity which indicates a severe oxidation of Ge at the HfO<sub>2</sub>-Si<sub>1-x</sub>Ge<sub>x</sub> interface after thermal annealing. On the other hand, for the annealed HfAlO film, there is only a small increment of the GeO<sub>x</sub> peak intensity, and the Ge peak is still higher than the GeO<sub>x</sub> peak, suggesting that adding alumina into HfO<sub>2</sub> suppresses further oxidation of Ge at the HfAlO-Si<sub>1-x</sub>Ge<sub>x</sub> interface. In addition, a very careful examination of the binding energy of the GeO<sub>x</sub> peak of the four samples reveals that there is a slightly higher energy shift ( $\sim 0.4$  eV) for the annealed HfAlO film [Fig. 1(b)(iv)] compared to the other three. The higher binding energy of Ge can be attributed to the more fully oxidized Ge,<sup>9</sup> and thus more energy is needed to break the bond resulting in a higher thermal stability and a lower diffusivity of Ge compared to GeO.<sup>16</sup> This Ge diffusion suppression effect is also revealed by the absence of a hysteresis loop in the following C-V result. It is interesting to note from Fig. 1(c), however, that this suppression effect is not that obvious for the formation of SiO<sub>x</sub> at the interface, suggesting that HfAlO may have some selectivity in suppressing the formation of GeO<sub>x</sub> and SiO<sub>x</sub> at the interfacial layer.

TEM images revealing the interfacial structures and reactions of the thin HfO<sub>2</sub> and HfAlO films on the strained Si<sub>1-x</sub>Ge<sub>x</sub> layer are shown in Fig. 2. It can be seen that after thermal annealing the interfacial layers formed at the HfO<sub>2</sub>-Si<sub>1-x</sub>Ge<sub>x</sub> interface for both the thinner and thicker films are relatively thicker and rougher compared to those at the HfAlO-Si<sub>1-x</sub>Ge<sub>x</sub> interface. This illustrates that the presence of alumina in the HfO<sub>2</sub> films helps to improve the interfacial structure during post thermal annealing. It is also worth noting that after annealing at 600 °C, the HfO<sub>2</sub> film is crystallized, while the HfAlO film remains amorphous. The existence of grain boundaries in the crystallized HfO<sub>2</sub> is believed to be responsible for the formation of a rougher interface

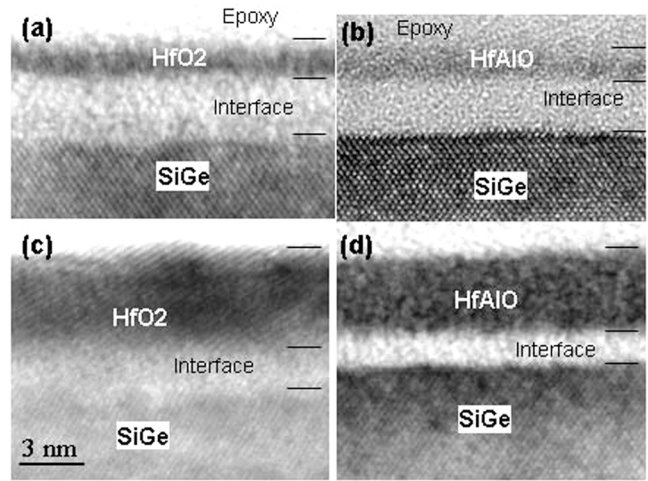


FIG. 2. (Color online) Cross-sectional TEM images showing the interfacial structures for the annealed samples of thin HfO<sub>2</sub> film (a), thin HfAlO film (b), thick HfO<sub>2</sub> film (c), and thick HfAlO film (d) on the compressively strained Si<sub>1-x</sub>Ge<sub>x</sub>.

since the oxygen diffusion along the grain boundaries is faster than that inside the grains.

Figure 3 shows the leakage current characteristics of the as-grown and annealed HfO<sub>2</sub> and HfAlO films on Si<sub>1-x</sub>Ge<sub>x</sub>. In general, the leakage current densities of HfAlO films are lower than those of HfO<sub>2</sub> films. The large decrease of the leakage current for the annealed films is attributed to the increase of the interfacial layer thickness and the reduction of oxygen deficiencies. The relatively larger leakage current for the annealed HfO<sub>2</sub> film compared to the annealed HfAlO film can be attributed to the crystallization of the HfO<sub>2</sub> oxide layer.<sup>5,18,19</sup>

Figure 4 shows characteristic C-V curves of the as-grown and annealed HfO<sub>2</sub> and HfAlO films on Si<sub>1-x</sub>Ge<sub>x</sub>. A significant change can be seen in Fig. 4(a) for the HfO<sub>2</sub> film after annealing. For the as-grown HfO<sub>2</sub> film, there is a large negative flat-band voltage shift ( $V_{FB}$ ) and a hysteresis loop during forward and reversed bias sweeps. The large negative shift indicates the existence of positive fixed charges in the HfO<sub>2</sub> film. The positive fixed charge in the HfO<sub>2</sub> films has been theoretically explained recently by Robertson<sup>20</sup> and has

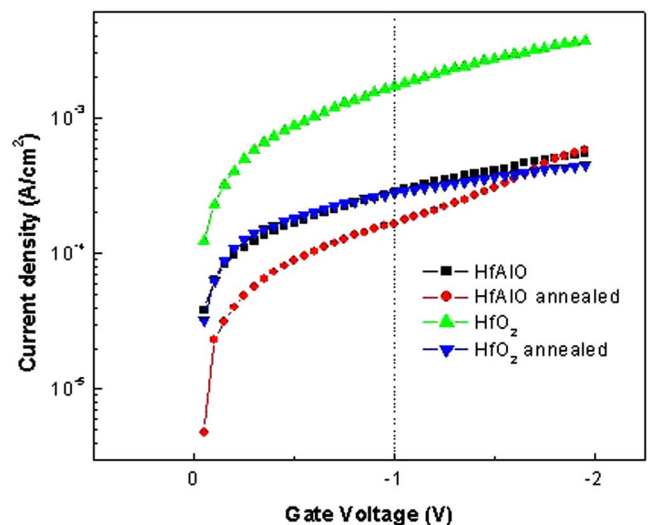


FIG. 3. (Color online)  $J$ - $V$  characteristics for the HfO<sub>2</sub> and HfAlO films before and after thermal annealing in a N<sub>2</sub> ambient at 600 °C for 45 min.

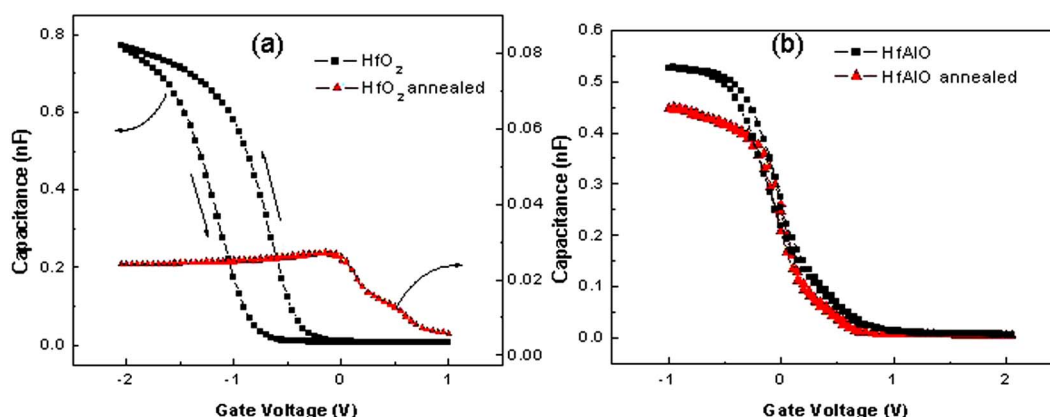


FIG. 4. (Color online)  $C$ - $V$  characteristics for  $\text{HfO}_2$  (a) and  $\text{HfAlO}$  films (b) before and after thermal annealing in a  $\text{N}_2$  ambient at  $600^\circ\text{C}$  for 45 min.

been attributed to oxygen vacancies. Therefore, the right shift of the  $C$ - $V$  curve after annealing can be explained as a result of the reduction of the number of oxygen vacancies in the  $\text{HfO}_2$  film. The large anticlockwise hysteresis loop presented in Fig. 4(a) indicates charge trapping in the oxide, and the diffusion of Ge into the oxide is believed to be responsible for the observed charge storages.<sup>4,19</sup> The oxide trapped charge density ( $N_{\text{ot}}$ ) can be calculated from the  $C$ - $V$  loop by the following formula:<sup>19</sup>

$$N_{\text{ot}} = \frac{C_{\text{acc}} \Delta V_{\text{FB}}}{qA},$$

where  $C_{\text{acc}}$  is the accumulation capacitance,  $\Delta V_{\text{FB}}$  is the hysteresis width,  $q$  is the electron charge, and  $A$  is the electrode area. The density of the trapped charges is calculated to be about  $7 \times 10^{12} \text{ cm}^{-2}$ . Although the hysteresis loop disappears after thermal annealing, the  $C$ - $V$  curve shows a large stretch-out, indicating the formation of high densities of interface traps. The significant decrease of the accumulation capacitance for the annealed  $\text{HfO}_2$  film is due to the formation of thick Si- and Ge-riched interfacial layers. In Fig. 4(b), however, the  $C$ - $V$  curve is normal with a very small flat-band voltage shift. The change of the accumulation capacitance of the  $\text{HfAlO}$  film after annealing is also very small, indicating a very small reduction of the dielectric constant of the film due to the relatively small increment of the  $\text{HfAlO-Si}_{1-x}\text{Ge}_x$  interfacial layer thickness. The effective dielectric constants (including the interfacial layer) of the as-grown and annealed  $\text{HfO}_2$  films derived from Fig. 4 are about 16 and 5, respectively, while they are 11 and 9, respectively, for the as-grown and annealed  $\text{HfAlO}$  films. It is apparent that adding alumina into  $\text{HfO}_2$  improves the interfacial property with a sacrificed value of the dielectric constant.

The merit of adding alumina in  $\text{HfO}_2$  can be considered in terms of the suppression of the interfacial reactions and Ge diffusion. The XPS and  $C$ - $V$  results suggest that the presence of alumina in the  $\text{HfO}_2$  films reduces the interfacial reaction, which is evidenced by the relatively lower Ge-O peak and smaller interfacial layer thicknesses and roughnesses. Even though TEM results do not show distinct differences in interfacial layer thickness, the fact of having less  $\text{GeO}_x$  presence in the XPS result and the disappearance of the hysteresis loop in the  $C$ - $V$  measurement suggest that adding

alumina in  $\text{HfO}_2$  may reduce the Ge diffusion into the dielectric layer, as alumina serves as an effective diffusion barrier.

In conclusion, the suppression of the  $\text{GeO}_x$  formation and the Ge diffusion has been achieved by adding alumina into the  $\text{HfO}_2$  gate dielectric film on the strained  $\text{Si}_{1-x}\text{Ge}_x$ . The corresponding electrical performance has also been improved, as evidenced by the decrease of the leakage current and charge traps in the dielectric layer.

This project is supported by the Hong Kong RGC grant (No. B-Q772).

- <sup>1</sup>G. D. Wilk, R. M. Wallace, and J. M. Anthony, *J. Appl. Phys.* **89**, 5243 (2001).
- <sup>2</sup>T. C. Chen, L. S. Lee, W. Z. Lai, and C. W. Liu, *Mater. Sci. Semicond. Process.* **8**, 209 (2005).
- <sup>3</sup>C. K. Maiti, S. K. Samanta, S. Chatterjee, G. K. Dalapati, and L. K. Bera, *Solid-State Electron.* **48**, 1369 (2004).
- <sup>4</sup>S. H. Jeong, Y. Roh, N. E. Lee, and C. W. Yang, *Surf. Coat. Technol.* **200**, 258 (2005).
- <sup>5</sup>J. H. Lee, S. Maikap, D. Y. Kim, R. Mahapatra, S. K. Ray, Y. S. No, and W. K. Choi, *Appl. Phys. Lett.* **83**, 779 (2003).
- <sup>6</sup>J. Kim, S. Kim, H. Jeon, M. H. Cho, K. B. Chung, and C. Bae, *Appl. Phys. Lett.* **87**, 053108 (2005).
- <sup>7</sup>P. F. Lee, J. Y. Dai, K. H. Wong, H. L. W. Chan, and C. L. Choy, *Appl. Phys. Lett.* **82**, 2419 (2003).
- <sup>8</sup>D. Y. Cho, K. S. Park, B. H. Choi, and S. J. Oh, *Appl. Phys. Lett.* **86**, 041913 (2005).
- <sup>9</sup>J. F. Damlencourt, O. Weber, O. Renault, J. M. Hartmann, C. Poggi, F. Ducroquet, and T. Billon, *J. Appl. Phys.* **96**, 5478 (2004).
- <sup>10</sup>M.-H. H. Tae-Hyoung Moon, *Appl. Surf. Sci.* **240**, 105 (2004).
- <sup>11</sup>M. S. Kim, Y. D. Ko, M. S. Yun, J. H. Hong, M. C. Jeong, J. M. Myoung, and I. G. Yun, *Mater. Sci. Eng., B* **123**, 20 (2005).
- <sup>12</sup>T. J. Park, S. K. Kim, J. H. Kim, J. Park, M. J. Cho, S. W. Lee, S. H. Hong, and C. S. Hwang, *Microelectron. Eng.* **80**, 222 (2005).
- <sup>13</sup>M. Houssa, B. De Jaeger, A. Delabie, S. Van Elshocht, V. V. Afanas'ev, J. L. Autran, A. Stesmans, M. Meuris, and M. M. Heyns, *J. Non-Cryst. Solids* **351**, 1902 (2005).
- <sup>14</sup>Z. H. Shi, D. Onsongo, and S. K. Banerjee, *Appl. Surf. Sci.* **224**, 248 (2004).
- <sup>15</sup>K. I. Seo, P. C. McIntyre, S. Sun, D. I. Lee, P. Pianetta, and K. C. Saraswat, *Appl. Phys. Lett.* **87**, 042902 (2005).
- <sup>16</sup>N. Lu, W. Bai, A. Ramirez, C. Mouli, A. Ritenour, M. L. Lee, D. Antoniadis, and D. L. Kwong, *Appl. Phys. Lett.* **87**, 051922 (2005).
- <sup>17</sup>H. Y. Yu, N. Wu, M. F. Li, C. X. Zhu, B. J. Cho, D. L. Kwong, C. H. Tung, J. S. Pan, J. W. Chai, W. D. Wang, D. Z. Chi, C. H. Ang, J. Z. Zheng, and S. Ramanathan, *Appl. Phys. Lett.* **81**, 3618 (2002).
- <sup>18</sup>V. Mikhelashvili, R. Brenner, O. Kreinin, B. Meyler, J. Shneider, and G. Eisenstein, *Appl. Phys. Lett.* **85**, 5950 (2004).
- <sup>19</sup>K. Kukli, M. Ritala, T. Sajavaara, J. Keinonen, and M. Leskelä, *Thin Solid Films* **416**, 72 (2002).
- <sup>20</sup>J. Robertson, *Solid-State Electron.* **49**, 283 (2005).